Desalination and Water Treatment
www.deswater.com

doi: 10.5004/dwt.2023.29960

310 (2023) 189–199
October

Study on factors affecting, isotherms, kinetics, thermodynamics, and optimization of chromium ion adsorption process in aqueous solution by modified mussel shells

Trinh Hoang Nghia[a], Nguyen Thuy Chinh[a,b,*], Nguyen Xuan Thai[a], Ngo Thi Cam Quyen[b,c], Thai Hoang[a,b,*]

[a]*Institute for Tropical Technology, Vietnam Academy of Science and Technology, 18 Hoang Quoc Viet, Cau Giay, Hanoi 100000, Vietnam, emails: ntchinh@itt.vast.vn (N.T. Chinh), hoangth@itt.vast.vn (T. Hoang), kingoffeeders@gmail.com (T.H. Nghia), nguyenthaicnkth@gmail.com (N.X. Thai)*

[b]*Graduate University of Science and Technology, Vietnam Academy of Science and Technology, 18 Hoang Quoc Viet, Cau Giay, Hanoi 100000, Vietnam, email: ntcquyen@ntt.edu.vn*

[c]*Institute of Environmental Sciences, Nguyen Tat Thanh University, 300A Nguyen Tat Thanh Street, Ward 13, District 4, Ho Chi Minh City, Viet Nam*

Received 14 June 2023; Accepted 10 September 2023

ABSTRACT

In this study, the adsorption of chromium(VI) ions using mussel shell samples modified with organic substances, including sodium dodecyl sulfate and ethylenediaminetetraacetic acid, was investigated. The optimal conditions for the Cr(VI) ion adsorption process using modified mussel shell powder, such as pH, temperature, and time, were determined using response surface methodology and the Box–Behnken model, combined with Design-Expert 11.1.0.1 software. The results indicated that the adsorption capacity of Cr(VI) ions in the initial solution tended to decrease sharply, from 67% to about 24%, as the initial content of Cr(VI) ions increased from 0.1 to 10 mg/L. A similar trend was also observed in the Cr(VI) ion adsorption process as the temperature of the solution increased. Moreover, the ability to remove Cr(VI) ions in different pH environments was also evaluated, and clear results showed that the removal ability was best at a neutral pH. The adsorption isotherms of Cr(VI) ions by powdered modified mussel shells were investigated using the Langmuir, Freundlich, Temkin, and Dubinin–Radushkevich isotherm models, and the equations were fitted statistically. Additionally, the kinetics of the Cr(VI) ion adsorption were assessed. Optimal adsorption conditions for the removal of Cr(VI) ions by modified mussel shells were found at a solution pH of 6.61, the temperature of 46.2°C, and the contact time of 2 h. The obtained results demonstrated the effective removal of Cr(VI) ions from mussel shell material after modification. These findings suggest that modified mussel shell powder is very promising and highly efficient for removing heavy metal ions from wastewater.

Keywords: Biosorbent; Modified mussel shells; Isotherms; Kinetics; Optimization; Thermodynamics

1. Introduction

Today's rapid growth in industry, agriculture, and services is causing water contamination from various sources, directly impacting the environment and human health. One of the most pressing issues is heavy metal pollution, which adversely affects people's quality of life, health, and way of life. Water basins near industrial parks, major towns, and mining areas often serve as sources of pollution. Heavy metals can bio-accumulate in the food chain and enter the human body, leading to adverse effects. Water pollution due to heavy metals has a detrimental impact on both species and human living conditions [1,2].

---

* Corresponding authors.

1944-3994/1944-3986 © 2023 Desalination Publications. All rights reserved.

The main sources of industrial effluent introducing chromium (Cr), a particularly prevalent and harmful heavy metal contaminant, into natural streams are varied. Due to its high solubility, hexavalent chromium is mostly found in the form of chromate (CrO_4^{2-}) and dichromate ($Cr_2O_7^{2-}$) ions, which can accumulate in the liver, stomach, and kidneys. Additionally, it can result in aberrant hematological functions, gastrointestinal and dermatological issues, and skin disorders [2]. Chromium levels in drinking water must be less than 0.02 mg/L to minimize or eliminate contaminants [2]. Therefore, it is crucial to treat water bodies contaminated with chromium. Recently, several studies have focused on the adsorption of Cr(VI) ions in water using adsorption materials based on metal–organic frameworks (MOFs). For instance, Miao et al. [3] manufactured Fe-MOF materials, while Liu et al. [4] created a zeolite/Fe_3O_4/chitosan material complex. These materials have shown remarkable efficiency in removing Cr(VI) ions from aquatic environments. The results have been consistently positive, indicating the potential for removing not only Cr(VI) ions but also other heavy metal ions in a simple and feasible manner. Additionally, some materials synthesized from natural sources have also proven to be efficient adsorbents [5,6]. Qin et al. [5] prepared a novel hierarchically porous carbon using seaweeds as a carbon source and applied this material to the removal of tetracycline from water. Elmolla et al. [7] used rice straw as a biosorbent for chromium removal from aqueous solutions.

However, the fabrication of such materials has been exceedingly complex and costly. Therefore, there has been a priority shift towards researching materials readily available in nature as safe biosorbents that exhibit excellent adsorption properties and environmental friendliness. Hu et al. [8] effectively utilized crayfish shell waste as an outstanding biosorbent for removing Cu(II) and Pb(II) ions from synthetic wastewater. Similarly, Moideen et al. [9] harnessed wasted cockle shells as natural absorbents for treating polluted river water. Mussel shells have garnered significant attention as they fulfill the aforementioned criteria. The discarded shells occupied space and emitted odors that disrupted the ecosystem. To counter this, mussel shells are being repurposed globally, either to create new mussel reefs or to reintroduce the shells into the water to promote the growth of native mussels. While mussel shells primarily consist of calcium carbonate, they also contain polysaccharides, minerals, and trace amounts of iron, copper, nickel, magnesium, calcium, and sodium [10]. Numerous scientists have employed mussel shell powders to effectively remove various pollutants from water, such as pigments like methylene blue (MB) [11] and antibiotics like tetracycline [12], yielding highly favorable results. Additionally, several studies have explored the use of mussel shell powders for adsorbing heavy metal ions in water, including As(III), Cd(II), Cu(II), and Zn(II) ions, and have consistently reported adsorption rates exceeding 85% within a few hours of testing [13,14]. This underscores the exceptional pollutant-removal capabilities of mussel shell materials. Furthermore, many research groups have highlighted the reusability of mussel shell materials, offering promising prospects for future applications [15,16].

While numerous studies have explored the removal of common heavy metal ions, such as Cr(VI) ions, the use of modified mussel shell materials in this context has not received significant attention. Moreover, some materials, when subjected to various denaturation processes, have demonstrated highly effective pollutant adsorption capabilities. Therefore, this study focuses on the utilization of modified mussel shell materials in these tests. Additionally, a similar study was conducted that involved evaluating undenatured and denatured oyster shells. The results indicated that the denatured sample exhibited superior Cr(VI) ions removal capabilities compared with the undenatured sample [17]. Mussel shell materials possess several advantages, including environmental friendliness, cost-effectiveness, and widespread availability. As such, the primary objective of this experiment was to assess the capacity of modified mussel shell powder to adsorb Cr(VI) ions from water. Furthermore, it was aimed at determining the optimal conditions for the Cr(VI) ions adsorption process in aqueous solutions and exploring adsorption isotherms, kinetics, and thermo-kinetics. These aspects represent the novel contributions of this study.

2. Materials and methods

2.1. Materials

The mussel shells were collected from a marine area located in Phu Yen Province, Vietnam, with coordinates at 12°09′N and 109°11′E. This sea area is part of the East Sea. The chemicals used in the study included: sodium hypochlorite solution (NaClO, 10%, a commercial product from China), potassium dichromate ($K_2Cr_2O_7$, purity > 99%, Merck, Singapore), sodium dodecyl sulfate (SDS, provided by Sigma-Aldrich, Singapore), ethylenediaminetetraacetic acid (EDTA, purity 99.4%, Sigma-Aldrich, Singapore), and 1,5-diphenylcarbazide (DPC, purity 98%, provided by Sigma-Aldrich, Singapore).

2.2. Treatment of mussel shell samples

Initially, the mussel shells (designated as MS) were cleaned by washing them with water two or three times after collection. To remove moss and organic residues from the shells, the MS samples were soaked in a 10% NaClO solution (with a solid/liquid ratio of 100/2,000 g/mL) for 48 h. Subsequently, these shells were dried at 100°C for 5–6 h until they reached a consistent weight. Following this, the shells were milled with distilled water for 48 h using a ball milling machine. The powdered mussel shell was crushed, rinsed with distilled water, filtered, and then dried at 105°C until it reached a constant weight. These powders were later treated with EDTA and SDS (with SDS used as a surfactant) in 20 mL of distilled water, maintaining a ratio of MS/EDTA/SDS at 10/1/0.2 (w/w/w), and the treatment was carried out at 60°C for 2 h. This process resulted in the production of modified mussel shell powders, denoted as m-MS. The m-MS powder exhibits a cubic shape with sizes ranging from 1 to 3 μm (Fig. 1). It possesses a specific surface area of 4.7038 m^2/g (BET) and an average pore diameter of 49.29 nm. This pore diameter is well-suited for the adsorption of Cr(VI) ions, as Cr(VI) ions have a Pauling radius of 52 pm. The water contact angle of m-MS is measured at 21.37°, indicating its hydrophilic property, rendering it suitable for the adsorption of Cr(VI) in water.

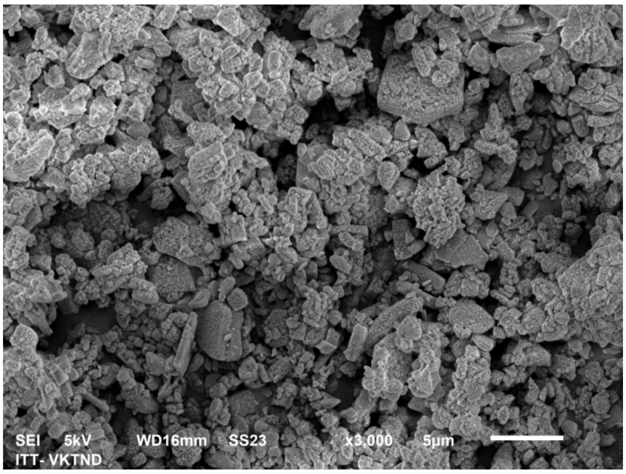

Fig. 1. Scanning electron microscopy image of m-MS.

In this study, the selection of substance ratios was based on the initial investigation results. Furthermore, it was observed that m-MS demonstrated significantly higher efficacy in removing Cr(VI) ions from an aqueous solution compared with the original MS sample without organic treatment. Therefore, the investigation into the effects of adsorption conditions and the optimization of the Cr(VI) ions adsorption process were exclusively conducted using the m-MS sample.

2.3. Experimental setup

2.3.1. Building calibration equation of Cr(VI) ions in water

To prepare the mother Cr(VI) solution (100 mg/L), 0.2829 g of $K_2Cr_2O_7$ was dissolved in 1 L of distilled water. Then, the mother solution was diluted with distilled water to obtain solutions with concentrations of 0.1, 0.5, 1, 5, and 10 mg/L, respectively. The optical adsorption value (Abs) of each solution was measured using an ultraviolet-visible (UV-Vis) spectrophotometer (CINTRA 40, GBC, USA). The calibration equation for Cr(VI) ions in an aqueous solution was determined as $y = 0.382x + 0.072$ and is illustrated in Fig. 2.

2.3.2. Chromium(VI) ion adsorption ability in aqueous solution by mussel shell powders

To create a 0.5% DPC solution, 0.4 g of DPC was completely dissolved in 100 mL of acetone solvent. After stirring, the solution was stored in a refrigerator at 4°C to protect it from light.

The process of Cr(VI) ion adsorption by the m-MS sample proceeded as follows: 0.2 g of m-MS powder was added to 50 mL of the Cr(VI) ion solution and shaken for 3 h using a shaking machine (IKA, Germany). Afterward, 10 mL of the filtered solution was extracted and transferred to a 50 mL beaker following filtration with filter papers. To this filtered solution, 1 mL of 1 M H_2SO_4 solution and 1 mL of DPC solution were added. The mixed solution was allowed to stand for 10 min to ensure a complete reaction between Cr(VI) ions and DPC, resulting in a reddish-purple solution. This solution was subsequently used to measure the absorbance of Cr(VI) ion solution using a UV-Vis spectrophotometer (CINTRA 40, GBC, USA) at a maximum wavelength of 540 nm [4,17].

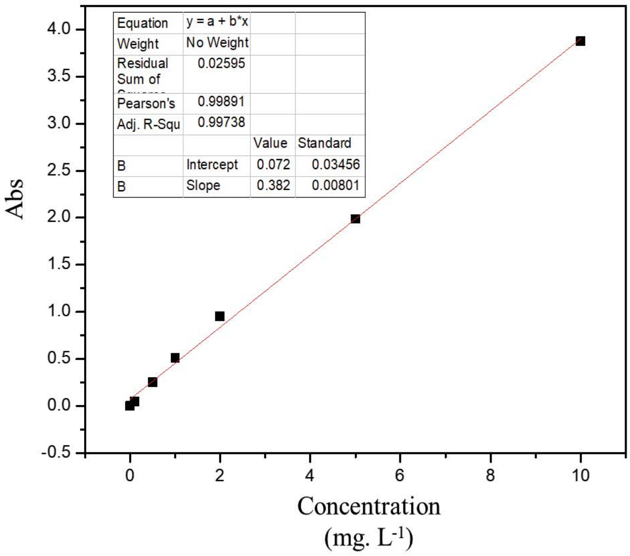

Fig. 2. Calibration equation of Cr(VI) ions in aqueous solution.

Eq. (1) was used to determine the quantity of Cr(VI) ions adsorbed per 1 g of adsorbent:

$$Q = \frac{\left(C_0 - C_e\right) \cdot V}{W} \tag{1}$$

where C_0 and C_e are the concentrations of Cr(VI) ion in solution at initial and equilibrium (mg/L), V is the volume of solution (L), W is the mass of the m-MS sample, and Q is the quantity of Cr(VI) ions adsorbed per gram of adsorbent at an equilibrium condition (g). The removal of Cr(VI) ion (H) was calculated using Eq. (2):

$$H = \frac{\left(C_0 - C_e\right)}{C_0} \times 100 \tag{2}$$

2.3.3. Optimization of adsorption process

The optimal conditions for the Cr(VI) ion adsorption process using the m-MS sample in this study were determined through the response surface method (RSM) using the Box–Behnken model and Design-Expert 11.1.0.1 software. Various process variables were investigated, including the pH of the medium, adsorption time, and adsorption temperature [18,19]. Two objective functions, denoted as H (Y_1) and Q (Y_2), were considered. For developing the experimental design based on the Box–Behnken model, a quadratic model was selected. The factors under investigation, with three levels each (base level (0), low level (−1), and high level (+1)), are the input parameters (Table 1). Additionally, there were five experiments conducted at the center.

Table 1
Experimental levels of technological variables

Real variable	Code variable	Range of variation (Δ)	Research level		
			–1	0	+1
Z1: Adsorption temperature (°C)	*A*	10	30	40	50
Z2: Adsorption time (h)	*B*	1	1	2	3
Z3: pH of the medium	*C*	3	4	7	10

3. Results and discussions

3.1. Effect of technological factors on Cr(VI) ion adsorption process

3.1.1. Effect of the pH medium

The impact of pH on the adsorption of Cr(VI) ions by the m-MS sample can be further elucidated by considering the presence of various chromium ions in solution ($HCrO_4^-$, $Cr_2O_4^{2-}$, and $Cr_2O_7^{2-}$) as well as the zero-point charge (pH_{pzc}) value of the m-MS sample. Surface hydroxyl groups and adsorbate anions in the aqueous phase can undergo protonation or deprotonation as the pH changes. In an acidic medium (pH 4), the dominant forms of Cr(VI) ions are the anions $HCrO_4^-$ and $Cr_2O_7^{2-}$, with $HCrO_4^-$ being the more prevalent. The pH_{pzc} value of the m-MS sample is 6.3. Therefore, when the solution pH is below 6.3, the surface of the m-MS sample becomes positively charged, leading to strong electrostatic attraction between the m-MS sample and Cr(VI) ions [18]. However, the primary components of MS powders, such as CaO and $CaCO_3$, can partially dissolve in an acidic environment, resulting in a reduction in the weight of the m-MS sample. This reduced the m-MS sample's effectiveness in adsorbing and removing Cr(VI) ions in the acidic environment [18]. When the pH of the solution falls within the range of 6 to 7, Cr(VI) ions exist primarily as anions $HCrO_4^-$, $Cr_2O_4^{2-}$, and $Cr_2O_7^{2-}$, and the surface charge of the m-MS sample approaches zero. Adsorption in this scenario primarily occurs due to physical interactions between the active groups on the m-MS sample's surface and Cr(VI) ions, leading to the adsorption of Cr(VI) ions into the micro-pores within the m-MS sample structure. Furthermore, the presence of active groups (such as carbonyl and sulfate groups) from EDTA and SDS on the m-MS sample's surface can facilitate the reduction of Cr(VI) to Cr(III). These factors contribute to the increased removal percentage of Cr(VI) ions by the m-MS sample in this pH range. In this case, the mechanism of Cr(VI) ions removal from the medium involves both reduction and anionic adsorption, with anionic adsorption being the dominant process due to electrostatic attraction and complex formation. At pH 10, Cr(VI) ion species predominantly exist as the anion CrO_4^{2-}, which carries the same negative charge as the m-MS sample. Consequently, the adsorption capacity of the m-MS sample for Cr(VI) ions is significantly reduced in a pH 10 solution [20].

The results in Fig. 3a demonstrates the percentage removal of Cr(VI) ions by the m-MS sample in the following order: pH 7 > pH 6 > pH 4 > pH 10. For instance, as the pH value increased from 7 to 10 (from a neutral to a basic condition), the percentage removal of Cr(VI) ions in the solution sharply decreased from 67.35% to 50.10%. Conversely, it increased significantly from 61.12% to 67.35% when the pH of the solution changed from acidic to neutral (from pH 4 to pH 7) after 3 h of testing. This result is consistent with findings from Yusuff [21], where mussel shell powders exhibited an increased ability to remove Cr(VI) ions as the pH of the medium increased from 2 to 7 (from 76% to 81%), but this ability tended to decrease as the pH value was further changed from 7 to 10. Similar pH-dependent trends were also observed in the results reported by Gupta et al. [22].

3.1.2. Effect of contact time

The results regarding the effect of adsorption time on the percentage removal of Cr(VI) ions by the m-MS sample are presented in Fig. 3b. The m-MS powder's ability to remove Cr(VI) ions increased from 24.49% to 69.39% as the adsorption duration was extended from 1 to 3 h. These experiments were conducted using a Cr(VI) ion solution with a concentration of 0.1 mg/L. It is evident that Cr(VI) ions were rapidly removed during the initial 2.5 h of testing, after which the rate of removal slowed down. This can be explained by the fact that the m-MS adsorbent's surface initially had numerous vacant sites, allowing for a rapid interaction between Cr(VI) ions and the m-MS sample. As adsorption proceeded, it eventually reached equilibrium, with the active sites of the m-MS adsorbent becoming fully saturated with Cr(VI) ions. Furthermore, when the adsorption time was extended from 1 to 3 h, an improvement in the removal of Cr(VI) ions from solutions with higher initial concentrations of 1 and 5 mg/L was observed. For instance, the removal efficiency of Cr(VI) ions from a 10 mg/L solution after 1 h was 8.94%, while after 2 and 3 h of testing, it increased to 31.56% and 34.94%, respectively. These findings align with results reported in references [22,23].

3.1.3. Effect of temperatures

The influence of temperature on the Cr(VI) ions adsorption process by the m-MS sample was investigated within a temperature range of 30°C to 50°C.

Fig. 3c illustrates that the removal efficiency of Cr(VI) ions from the aqueous solution increased from 65.31% to 69.39% when the temperature was raised from 30°C to 50°C after 3 h of testing. This increase in removal efficiency with higher temperatures was also observed for different durations. The adsorption temperature had a favorable effect on the m-MS powder's ability to remove Cr(VI) ions from the aqueous solution, indicating that the surface of the m-MS powders had more active sites. Additionally, at higher temperatures, Cr(VI) ions were more widely dispersed in the solution, making it easier for the m-MS powders to adsorb [24].

3.1.4. Effect of initial Cr(VI) concentration

The effect of the initial concentrations of the Cr(VI) ions solution on the m-MS sample's ability to adsorb Cr(VI) ions was evaluated at a pH of 7 and an adsorption temperature of 40°C, as shown in Fig. 3d. It's evident that the ability to remove Cr(VI) ions decreased significantly after 3 h of testing, dropping from 67.35% to 34.40%, with an increase in the initial Cr(VI) concentration from 0.1 to 10 mg/L (Fig. 3d). Conversely, the m-MS sample exhibited greater adsorption of Cr(VI) ions in the aqueous solution at lower initial concentrations of Cr(VI) ions. This can be attributed to the significant increase in the initial Cr(VI) ions concentration, which led to the surface saturation of the adsorbent and resulted in a significant decline in the removal of Cr(VI) ions. These results align with previous reports [25,26].

3.2. Adsorption isotherms data analysis

Adsorption isotherm models have been employed to study the adsorption mechanisms at equilibrium. Fig. 4 depicts the fitting of the Freundlich, Langmuir, Temkin, and Dubinin–Radushkevich isotherm models based on the data from subsection 3.1. The regression coefficient (R^2) values are used to determine the most suitable isotherm model for adsorption. Both the Langmuir and Freundlich adsorption isotherm models exhibited excellent agreement with the experimental data, with R^2 values higher than 0.99 [27]. The fitting curve based on the Langmuir adsorption isotherm model had a slightly higher R^2 value than that of the Freundlich adsorption isotherm model. The Langmuir adsorption isotherm model describes the monolayer adsorption of adsorbate atoms (molecules, ions) on a flat surface, while the Freundlich isotherm model is used to depict multi-faceted adsorption on an adsorbent with a heterogeneous surface. This suggests that m-MS samples possess reliable adsorption sites that enable the formation of a monolayer of anion species. Similar findings have been reported for the removal of Cr(VI) ions from aqueous solutions using peanut shells and bamboo waste, both of which followed the Langmuir adsorption isotherm model [25,28–31].

3.3. Adsorption kinetics

In this study, four kinetic equations—first-order, second-order, pseudo-first-order, and pseudo-second-order—were fitted to the obtained data and compared with determine which equation best described the Cr(VI) ions adsorption process by m-MS powders. The kinetic analysis was conducted at an initial Cr(VI) ions concentration of 1 mg/L and a temperature of 40°C. The four models for Cr(VI) ions adsorption onto m-MS powders were fitted linearly, as shown in Fig. 5. The choice of the most suitable equation was based on the regression coefficient (R^2). The values of R^2 were higher than 0.970 for all kinetic models. Among them, the pseudo-second-order kinetic equation was

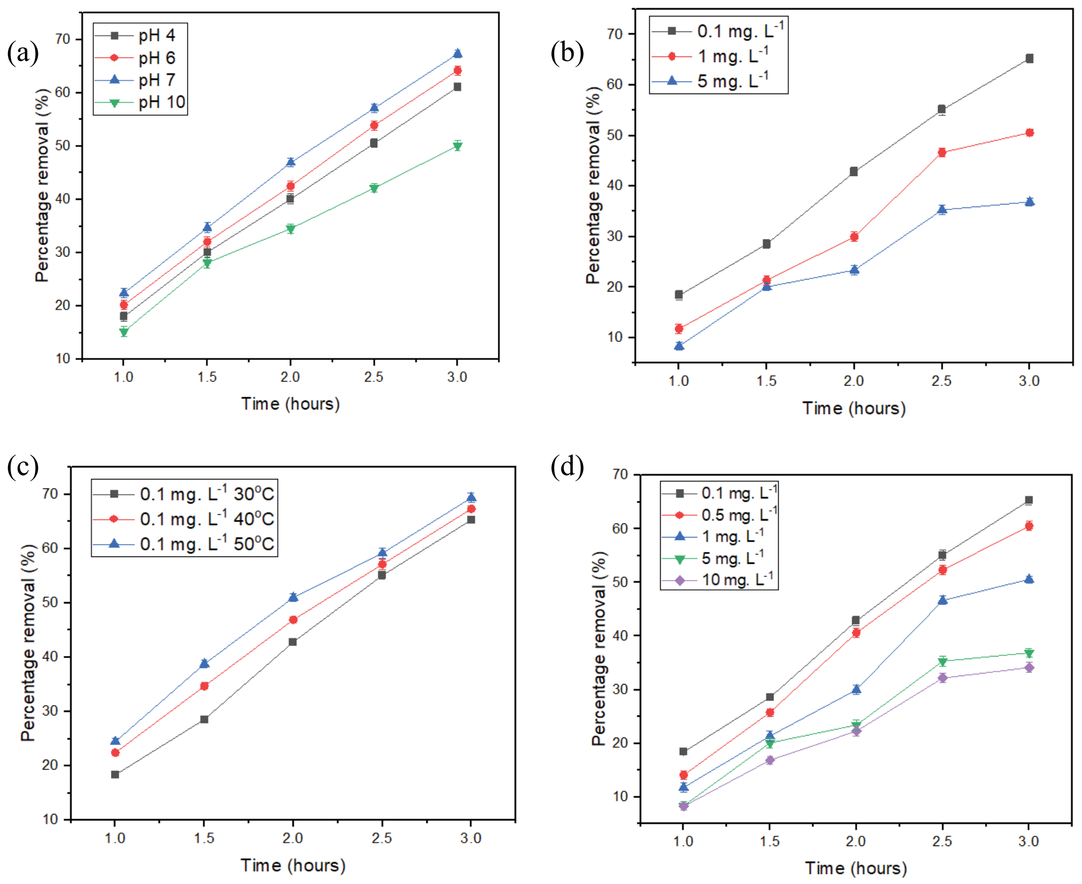

Fig. 3. Percentage of removed Cr(VI) ions by m-MS powders in different pH medium (a), different testing time (b), different temperature (c), and different initial Cr(VI) ions concentration (d).

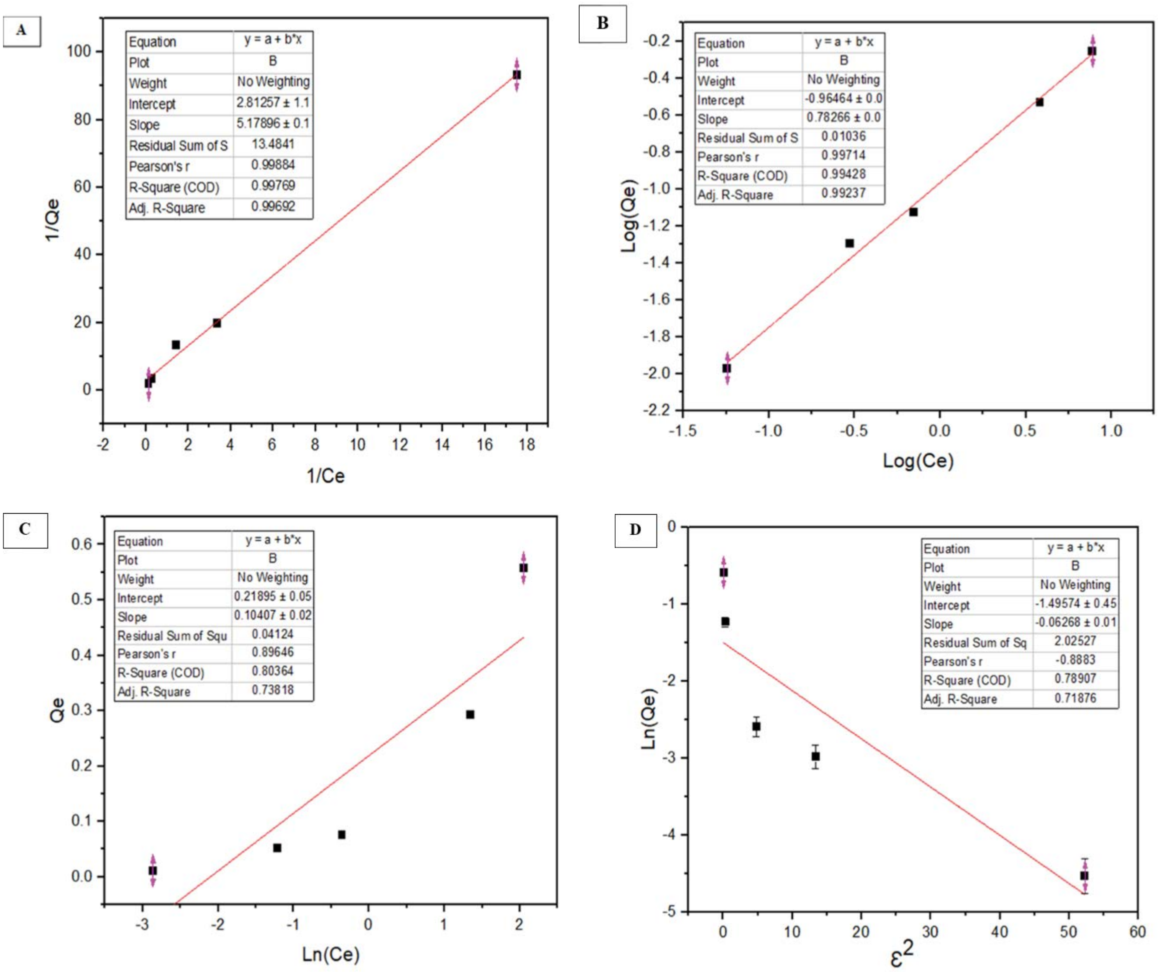

Equation	y = a + b*x
Plot	B
Weight	No Weighting
Intercept	2.81257 ± 1.1
Slope	5.17896 ± 0.1
Residual Sum of S	13.4841
Pearson's r	0.99884
R-Square (COD)	0.99769
Adj. R-Square	0.99692

Equation	y = a + b*x
Plot	B
Weight	No Weighting
Intercept	-0.96464 ± 0.0
Slope	0.78266 ± 0.0
Residual Sum of S	0.01036
Pearson's r	0.99714
R-Square (COD)	0.99428
Adj. R-Square	0.99237

Equation	y = a + b*x
Plot	B
Weight	No Weighting
Intercept	0.21895 ± 0.05
Slope	0.10407 ± 0.02
Residual Sum of Squ	0.04124
Pearson's r	0.89646
R-Square (COD)	0.80364
Adj. R-Square	0.73818

Equation	y = a + b*x
Plot	B
Weight	No Weighting
Intercept	-1.49574 ± 0.45
Slope	-0.06268 ± 0.01
Residual Sum of Sq	2.02527
Pearson's r	-0.8883
R-Square (COD)	0.78907
Adj. R-Square	0.71876

Fig. 4. Different isotherm models with their equations and correlation coefficient values (a) Langmuir, (b) Freundlich, (c) Temkin, and (d) Dubinin–Radushkevich isotherms.

the best fit for the experimental data (R^2 = 0.99). Therefore, it can be suggested that the pseudo-second-order kinetic equation is appropriate for describing the Cr(VI) ion adsorption process by the m-MS sample, and the adsorption is of the chemisorption type, which is consistent with previous findings published by Alshammari et al. [32].

3.4. Thermodynamics of adsorption

The free energy change $\Delta G° = -RT\ln(K)$ [Eq. (3)] of Cr(VI) ion adsorption process:

$$\ln\left(K\right) = -\frac{\Delta H}{R}\frac{1}{T} + \frac{\Delta S}{R} \tag{3}$$

where R is the universal gas constant (R = 8.314 J/mol·K), K is the thermodynamic equilibrium constant and T is the absolute temperature (K).

Since the adsorption of Cr(VI) ions by m-MS powders was consistent with the Langmuir isotherm adsorption, the K parameters were calculated based on this equation by extrapolating to zero. The Langmuir equation is presented as follows: $y = 5.178x + 2.812$.

It can be calculated enthalpy: $\Delta H°$ = –5.178 × 8.314 = –43.04 (J/mol), and entropy $\Delta S°$ = 2.812 × 8.314 = 23.37 (J/mol·K).

The values of $\Delta G°$ for the Cr(VI) ion adsorption process on the m-MS sample were calculated and found to be –7,038; –7,273 and –7,508 J/mol at 303, 313, and 323 K, respectively. A negative $\Delta G°$ value indicates that the Cr(VI) ion adsorption process on the m-MS sample can occur spontaneously under natural conditions without the need for any catalysts. The positive $\Delta S°$ value suggests that m-MS powders have a strong affinity for adsorbing Cr(VI) ions onto their surface, and that there may be a structural change during the adsorption process [33,34].

3.5. Optimization of Cr(VI) adsorption process

In this study, various process parameters such as temperature, time, pH, and concentration were investigated to understand their influence on the adsorption of Cr(VI) ions by m-MS powder. Through preliminary research, it was identified that there are three crucial process parameters, denoted as A, B, and C, that significantly affect the adsorption of Cr(VI) ions by m-MS powder. These parameters are adsorption temperature (in °C), adsorption time (in hours),

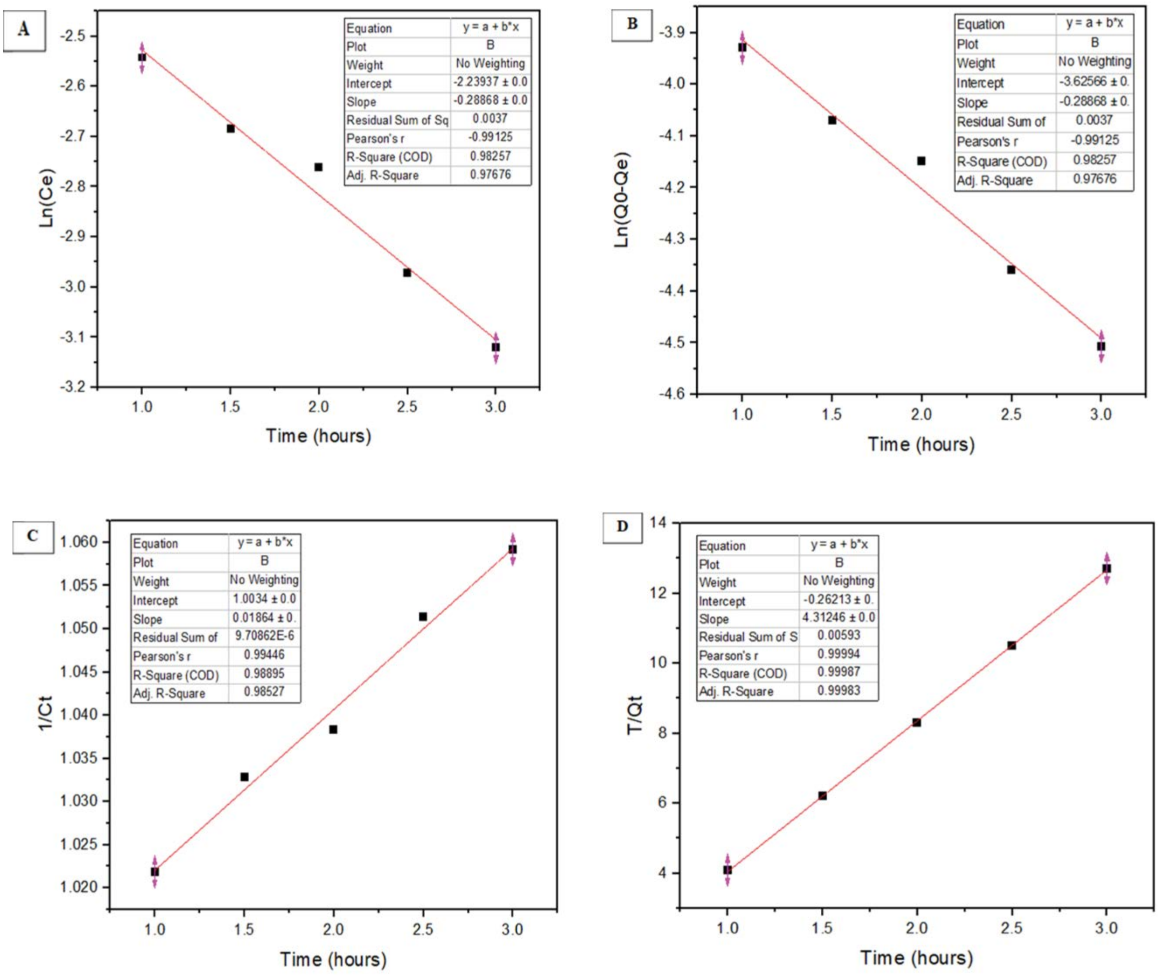

Fig. 5. Different linear kinetic models of Cr(VI) ions (a) first-order reaction, (b) pseudo-first-order reaction, (c) second-order reaction, (d) pseudo-second-order reaction adsorption according to their equations and correlation coefficient values.

and solution pH. To analyze the impact of these parameters on the adsorption performance and capacity, response surface methodology was used in conjunction with the Box–Behnken design. We defined two objective functions, H (percentage of Cr(VI) ions removed, Y_1) and Q (amount of Cr(VI) ions adsorbed per unit of adsorbent at equilibrium, Y_2). The factors were set at three levels: base level (0), low level (−1), and high level (+1), with $k = 3$ factors in total. Using Design-Expert software version 11.1.0.1, an experimental matrix plan and the optimal conditions were determined from the results of 17 experiments, as detailed in Table 2.

The model's compatibility was assessed through predicted vs. actual value plots and the residuals vs. runs models, as shown in Fig. 6. The model demonstrated a strong correlation between experimental and theoretical values, with the experimental points closely clustered along a straight diagonal line in the first graph. In the second graph, the distribution of experimental points appeared random within the range of (−8, 8) and (−6, 6).

The response surfaces for the Y_1 and Y_2 objective functions, in relation to pairs of technical factors, are depicted in Fig. 7. The dark red zone represents the ideal range, while the yellow, green, and blue areas indicate decreasing target function values. Both Y_1 and Y_2 exhibit their highest values within this zone [33–36].

The target functions are Y_1 (%): adsorption performance, and Y_2 (mg/g): adsorption capacity, respectively:

H (Y_1): the percentage of removed Cr(VI) ions (level 5)

Q (Y_2): the amount of Cr(VI) ions adsorbed per amount of adsorbent at equilibrium condition (level 3)

$$Y_1 = 34.506 + 17.28A + 2.7175B - 6.058C^2 \tag{4}$$

$$Y_2 = 0.088 + 0.04375A + 0.00625B - 0.005C - 0.01525C^2 \tag{5}$$

The Design-Expert 11.1.0.1 program identified one solution, corresponding to a set of ideal technological data, as shown in Table 3. Under these optimal conditions, the predicted values for the objective functions are H = 54.13% and Q = 0.14 mg/g.

To validate the optimization process, experiments were conducted in three replicates under the optimal conditions: an adsorption temperature of 46.2°C, an initial Cr(VI) ion concentration of 1 mg/L, an adsorption time of 2 h, and an adsorption pH of 6.61. The obtained values for H and Q were 52.09% ± 0.13% and 0.13 ± 0.04 mg/g, respectively.

Table 2
Data setup of optimization process

No	Code variable			Objective function	
	A	*B*	*C*	Y_1 (mg GAE/g)	Y_2 (%)
1	1	1	0	55.88	0.14
2	1	0	–1	47.77	0.12
3	–1	0	–1	15.55	0.04
4	–1	0	1	12.51	0.03
5	–1	1	0	21.37	0.05
6	0	–1	–1	26.13	0.07
7	0	0	0	33.33	0.08
8	0	1	–1	30.07	0.08
9	1	0	1	45.19	0.11
10	0	1	1	27.42	0.07
11	0	0	0	35.12	0.09
12	0	–1	1	24.52	0.06
13	0	0	0	34.82	0.09
14	0	0	0	35.01	0.09
15	–1	–1	0	11.76	0.03
16	1	–1	0	50.59	0.13
17	0	0	0	34.25	0.09

These values closely matched the predicted values of *H* (54.13%) and *Q* (0.14 mg/g), indicating that the experimental results for m-MS powders in this study align with the optimized computational model. It's worth noting that this material may not be as efficient as some previously published materials, such as granular and powdered *Peganum harmala* or porous carbon derived from corn straw, which can achieve removal efficiencies of up to 80% or 90% under conditions of relatively high contaminant concentration [36,37]. It offers the advantages of being environmentally friendly, readily available, easy to process, and cost-effective.

The experiment was carried out at optimal conditions (the adsorption time of 2 h, the adsorption pH of 6.61, the temperature of 46.2°C, the concentration of initial Cr(VI) ion solution varied from 1, 2, 5, 10, and 15 mg/L) to find the maximum monolayer adsorption capacity (Q_{max}) for Cr(VI) ion removal process using modified mussel shells. Fig. 8 presents the data were fitted by Langmuir isotherm model with the equation in the form: $y = 4.7454x + 0.0703$ ($R^2 = 0.9946$). From this model, it can be calculated that the Q_{max} for Cr(VI) ion removal process using modified mussel shells reached 14.22 mg/g. As can be compared with similar adsorbents in Table 4, the modified mussel shells in this study have a great Cr(VI) ion adsorption ability.

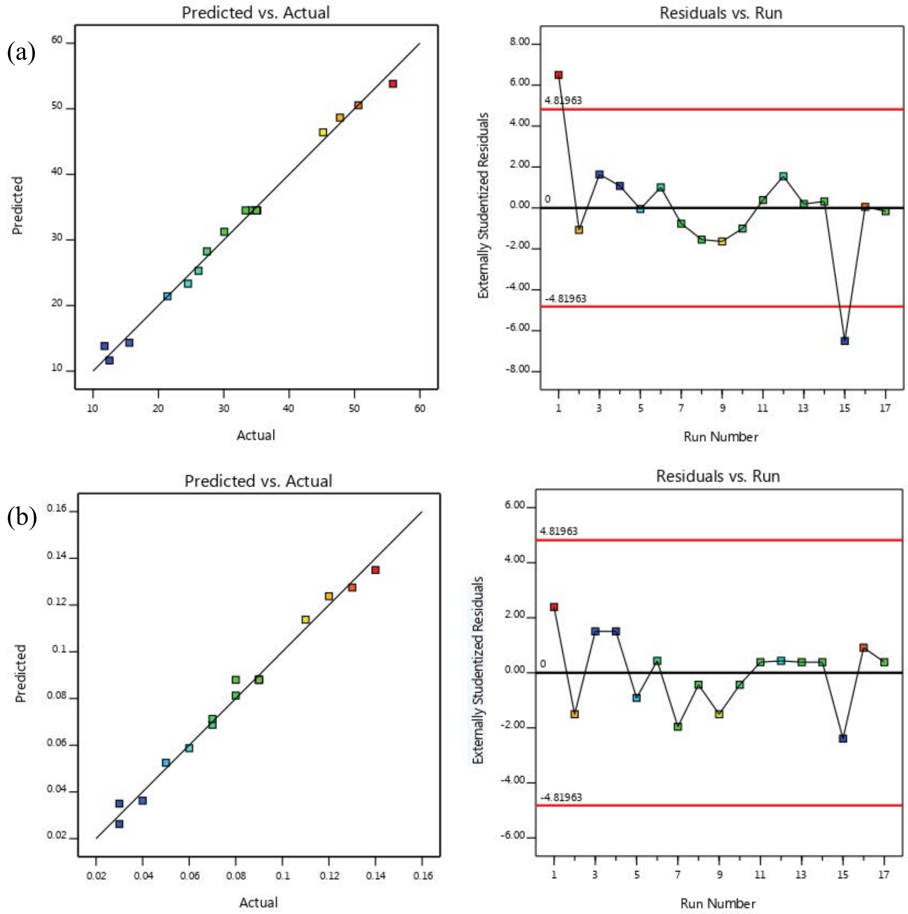

Fig. 6. Empirical and predictive charts, random distributions of Y_1 (a) and Y_2 (b).

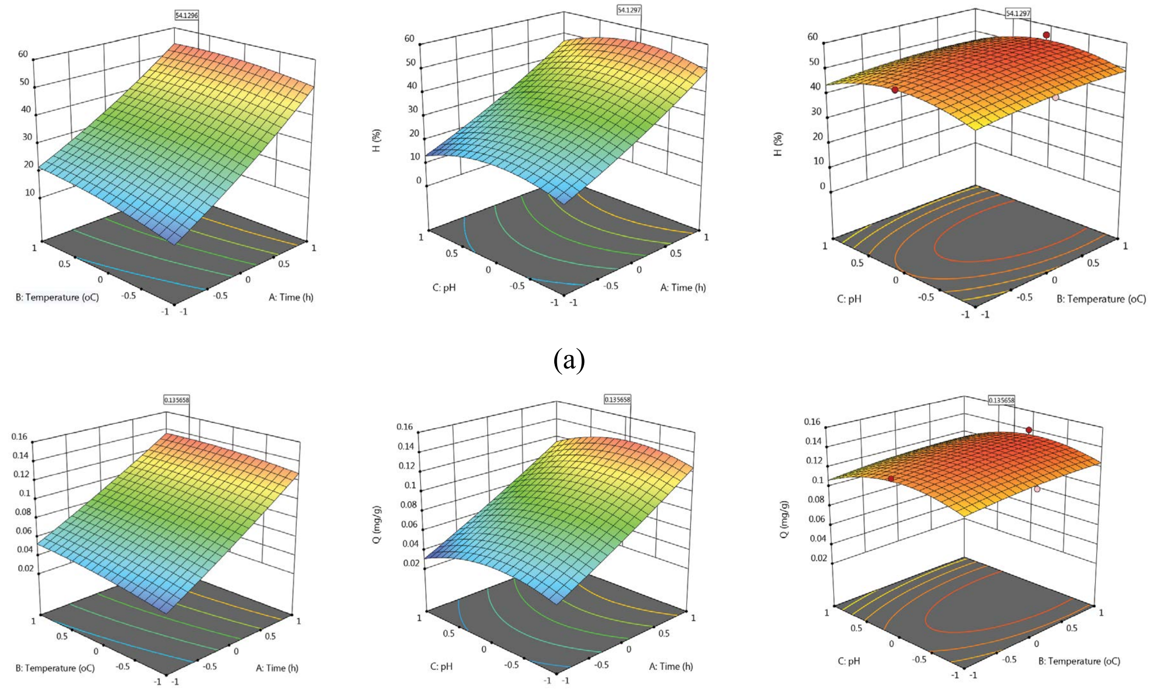

(a)

(b)

Fig. 7. Surface response of adsorption performance Y_1 (a) and adsorption capacity Y_2 (b).

Table 3
Empirical results of target functions at optimal condition

Technological parameters			Objective function	Results	
Time (h)	Temperatures	pH		Experiments	Theoretical
2	46.2	6.61	Y_1 Y_2	52.09 ± 0.13 (%) 0.13 ± 0.04 (mg/g)	54.13 (%) 0.14 (mg/g)

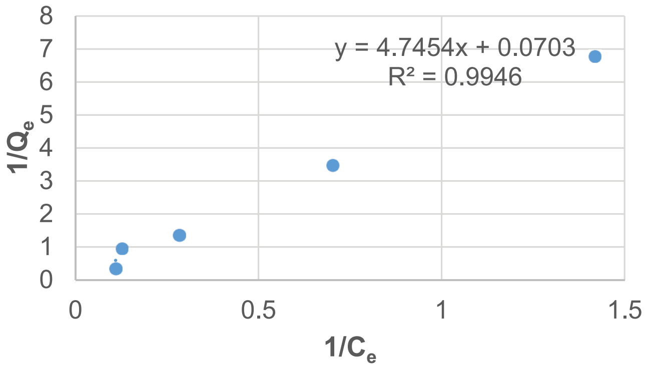

Fig. 8. Langmuir isotherm model with its equations and correlation coefficient value.

Table 4
Cr(VI) ion adsorption capacity of some absorbents from mussel shells

No.	Absorbent	Q_{max} (mg/g)	References
1	Different treatment rice straw	7.99–40.32	[7]
2	Acid treated snail shell powder	10.69	[29]
3	Groundnut shell	3.79	[30]
4	Sugarcane bagasse	1.76	[31]
5	Modified mussel shell powder	14.22	Present work

4. Conclusions

In conclusion, various environmental factors, such as solution pH, temperature, reaction duration, and initial Cr(VI) ion concentration, were evaluated for their impact on the adsorption capacity of Cr(VI) ions by m-MS powders. With the exception of the initial concentration of Cr(VI) ions solution, which showed a significant decrease in percentage removal as it increased from 0.1 to 10 mg/L, most parameters had a favorable effect on the removal of Cr(VI) ions, particularly temperature and reaction duration. The Langmuir isotherm and pseudo-second-order kinetic model provided the most accurate descriptions of the adsorption isotherm and kinetics, with correlation coefficients (R^2) of approximately 0.99 each. Optimal conditions for Cr(VI) ion adsorption by the m-MS sample were determined using Design-Expert 11.1.0.1 and the Box–Behnken model, resulting in an ideal set of parameters: a temperature of 46.2°C, a solution pH of 6.61, and an adsorption time of 2 h. Under these conditions, the material exhibited excellent performance, removing up to 54.13% of Cr(VI) ions from the initial solution at a concentration of 1 mg/L after 2 h of contact. The maximum monolayer adsorption capacity for Cr(VI) ion removal process using modified mussel shells reaches 14.22 mg/g, suggesting that modified mussel shells are promising for the removal of heavy metal ions in water.

Acknowledgment

This research was funded by the Vietnam Academy of Science and Technology under grant number NCVCC13.01/22-23.

Credit authorship contribution statement

Trinh Hoang Nghia: Investigation, Formal analysis, Writing-original draft preparation. Nguyen Thuy Chinh: Methodology, Writing-Reviewing, and Editing, Supervision. Nguyen Xuan Thai: Formal analysis, Investigation. Ngo Thi Cam Quyen: Validation. Thai Hoang: Scientific idea, Conceptualization, Funding acquisition, Writing-Reviewing, and Editing.

Declaration of competing interest

The authors declare that they have no known competing financial interests or personal relationships that could have appeared to influence the work reported in this paper.

References

[1] R. Rizk, T. Juzsakova, M.B. Ali, M.A. Rawash, E. Domokos, A. Hedfi, M. Almalki, F. Boufahja, H.M. Shafik, A. Rédey, Comprehensive environmental assessment of heavy metal contamination of surface water, sediments and Nile Tilapia in Lake Nasser, Egypt, J. King Saud Univ. Sci., 34 (2022) 101748, doi: 10.1016/j.jksus.2021.101748.

[2] C.Y. Gong, Z.G. Geng, A.L. Dong, X.X. Ye, G.Z. Wang, Y.X. Zhang, Highly efficient and selective removal of Pb(II) ions by sulfur-containing calcium phosphate nanoparticles, Chin. J. Chem. Phys., 29 (2016) 607–616.

[3] S. Miao, J. Guo, Z. Deng, J. Yu, Y. Dai, Adsorption and reduction of Cr(VI) in water by iron-based metal–organic frameworks (Fe-MOFs) composite electrospun nanofibrous membranes, J. Cleaner Prod., 370 (2022) 133566, doi: 10.1016/j.jclepro.2022.133566.

[4] X. Liu, Y. Zhang, Y. Liu, T. Zhang, Removal of Cr(VI) and Ag(I) by grafted magnetic zeolite/chitosan for water purification: synthesis and adsorption mechanism, Int. J. Biol. Macromol., 222 (2022) 2615–2627.

[5] W.X. Qin, N. Sun, G.Z. Wang, H.M. Zhang, Y.X. Zhang, Seaweed-derived hierarchically porous carbon for highly efficient removal of tetracycline, Chin. J. Chem. Phys., 35 (2022) 578–588.

[6] I. Zinicovscaia, L. Cepoi, T. Chiriac, O.A. Culicov, M. Frontasyeva, S. Pavlov, E. Kirkesali, A. Akshintsev, E.R. Altmetric, *Spirulina platensis* as biosorbent of chromium and nickel from industrial effluents, Desal. Water Treat., 57 (2016) 11103–11110.

[7] E.S. Elmolla, W. Hamdy, A. Kassem, A.A. Hady, Comparison of different rice straw-based adsorbents for chromium removal from aqueous solutions, Desal. Water Treat., 57 (2016) 6991–6999.

[8] W.Q. Hu, S. Chen, H. Jiang, Crayfish shell waste as safe biosorbent for removal of Cu^{2+} and Pb^{2+} from synthetic wastewater, Chin. J. Chem. Phys., 35 (2022) 842–852.

[9] S.N.F. Moideen, M.F. Md. Din, M. Ponraj, M.B.M. Yusof, Z. Ismail, A.R. Songip, S. Chelliapan, Wasted cockle shell (*Anadara granosa*) as a natural adsorbent for treating polluted river water in the fabricated column model (FCM), Desal. Water Treat., 57 (2016) 16395–16403.

[10] J.L. Osa, G. Mondragon, N. Ortega, F.F. Marzo, C. Peña-Rodriguez, On the friability of mussel shells as abrasive, J. Cleaner Prod., 375 (2022) 134020, doi: 10.1016/j.jclepro.2022.134020.

[11] L. Wu, X. Zhang, J.A. Thorpe, L. Li, Y. Si, Mussel-inspired polydopamine functionalized recyclable coconut shell derived carbon nanocomposites for efficient adsorption of methylene blue, J. Saudi Chem. Soc., 24 (2020) 642–649.

[12] M. Conde-Cid, G. Ferreira-Coelho, M. Arias-Estévez, C. Álvarez-Esmorís, J.C. Nóvoa-Muñoz, A. Núñez-Delgado, M.J. Fernández-Sanjurjo, E. Álvarez-Rodríguez, Competitive adsorption/desorption of tetracycline, oxytetracycline and chlortetracycline on pine bark, oak ash and mussel shell, J. Environ. Manage., 250 (2019) 109509, doi: 10.1016/j.jenvman.2019.109509.

[13] C. Osorio-López, N. Seco-Reigosa, B. Garrido-Rodríguez, L. Cutillas-Barreiro, M. Arias-Estévez, M.J. Fernández-Sanjurjo, E. Álvarez-Rodríguez, A. Núñez-Delgado, As(V) adsorption on forest and vineyard soils and pyritic material with or without mussel shell: kinetics and fractionation, J. Taiwan Inst. Chem. Eng., 45 (2014) 1007–1014.

[14] B. Garrido-Rodriguez, L. Cutillas-Barreiro, D. Fernández-Calviño, M. Arias-Estévez, M.J. Fernández-Sanjurjo, E. Álvarez-Rodríguez, A. Núñez-Delgado, Competitive adsorption and transport of Cd, Cu, Ni, and Zn in a mine soil amended with mussel shell, Chemosphere, 107 (2014) 379–385.

[15] A. Prihanto, D.F. Fitriyana, S. Muryanto, I. Masykur, R. Ismail, J. Jamari, A.P. Bayuseno, Aqueous crystallization of monocalcium phosphate monohydrate with green mussel shells (*Verna piridis*) for calcium sources, J. Environ. Chem. Eng., 9 (2021) 106913, doi: 10.1016/j.jece.2021.106913.

[16] C. Martínez-García, B. González-Fonteboa, D. Carro-López, J.L. Pérez-Ordóñez, Assessment of mussel shells building solutions: a real-scale application, J. Build. Eng., 44 (2021) 102635, doi: 10.1016/j.jobe.2021.102635.

[17] T.C. Nguyen, X.T. Nguyen, D.M.T. Tran, Q.T. Vu, V.H. Nguyen, D.T. Nguyen, M.T. Do, T.L. Nguyen, T.N.L. Ly, H. Thai, Adsorption ability for toxic chromium(VI) ions in aqueous solution of some modified oyster shell types, Bioinorg. Chem. Appl., 2020 (2020) 1–17.

[18] N. Altunay, A. Elik, M. Tuzen, M.F. Lanjwani, M.R.A. Mogaddam, Determination and extraction of acrylamide in processed food samples using alkanol-based supramolecular solvent-assisted dispersive liquid-liquid microextraction coupled with spectrophotometer: optimization using factorial design, J. Food Compost. Anal., 115 (2023) 105023, doi: 10.1016/j.jfca.2022.105023.

[19] T. Dannen, B. Schindele, M. Prümmer, K. Arntz, T. Bergs, Methodology for the self-optimizing determination of additive manufacturing process eligibility and optimization potentials in toolmaking, Procedia CIRP, 107 (2022) 1539–1544.

[20] F. Echabbi, M. Hamlich, S. Harkati, A. Jouali, S. Tahiri, S. Lazar, R. Lakhmiri, M. Safi, Photocatalytic degradation of methylene blue by the use of titanium-doped calcined mussel shells CMS/TiO_2, J. Environ. Chem. Eng., 7 (2019) 103293, doi: 10.1016/j.jece.2019.103293.

[21] A.S. Yusuff, Adsorption of hexavalent chromium from aqueous solution by *Leucaena* leucocephala seed pod activated carbon: equilibrium, kinetic and thermodynamic studies, Arabian J. Basic Appl. Sci., 26 (2019) 89–102.

[22] V.K. Gupta, A. Rastogi, A. Nayak, Adsorption studies on the removal of hexavalent chromium from aqueous solution using a low-cost fertilizer industry waste material, J. Colloid Interface Sci., 342 (2010) 135–141.

[23] A.S. Yusuff, M.A. Lala, K.A. Thompson-Yusuff, E.O. Babatunde, $ZnCl_2$-modified eucalyptus bark biochar as adsorbent: preparation, characterization and its application in adsorption of Cr(VI) from aqueous solutions, S. Afr. J. Chem. Eng., 42 (2022) 138–145.

[24] F. Gorzin, M.B.R. Abadi, Adsorption of Cr(VI) from aqueous solution by adsorbent prepared from paper mill sludge: kinetics and thermodynamics studies, Adsorpt. Sci. Technol., 36 (2018) 149–169.

[25] M. Gazi, A.A. Oladipo, K.A. Azalok, Highly efficient and magnetically separable palm seed-based biochar for the removal of nickel, Sep. Sci. Technol., 53 (2018) 1124–1131.

[26] Z.A.A. Othman, R. Ali, M. Naushad, Hexavalent chromium removal from aqueous medium by activated carbon prepared from peanut shell: adsorption kinetics, equilibrium and thermodynamic studies, Chem. Eng. J., 184 (2012) 238–247.

[27] T.U.H. Shah, M.H. Tahir, A. Rahman, H.W. Liu, Superabsorbent capability and high retention ability of China clay (kaolinite)/polyacrylic acid composites for aqueous solution, Chin. J. Chem. Phys., 32 (2019) 508–512.

[28] T. Dula, K. Siraj, S.A. Kitte, Adsorption of hexavalent chromium from aqueous solution using chemically activated carbon prepared from locally available waste of bamboo (*Oxytenanthera abyssinica*), Int. Sch. Res. Notices, 2014 (2014) 438245, doi: 10.1155/2014/438245.

[29] X.H. Vu, L.H. Nguyen, H.T. Van, D.V. Nguyen, T.H. Nguyen, Q.T. Nguyen, L.T. Ha, Adsorption of chromium(VI) onto freshwater snail shell-derived biosorbent from aqueous solutions: equilibrium, kinetics, and thermodynamics, J. Chem., 2019 (2019) 3038103, doi: 10.1155/2019/3038103.

[30] J. Bayuo, K.B. Pelig-Ba, M.A. Abukari, Adsorptive removal of chromium(VI) from aqueous solution unto groundnut shell, Appl. Water Sci., 9 (2019) 107, doi: 10.1007/s13201-019-0987-8.

[31] I.D.L.C. Alomá, I. Rodríguez, M. Calero, G. Blázquez, Biosorption of Cr^{6+} from aqueous solution by sugarcane bagasse, Desal. Water Treat., 52 (2013) 5912–5922.

[32] M.S. Alshammari, I.M. Ahmed, J.S. Alsharari, I.H. Alsohaimi, N.S. Al-Muaikel, T.S. Alraddadi, T.H.A. Hasanin, Adsorption of Cr(VI) using α-Fe_2O_3 coated hydroxy magnesium silicate (HMS): isotherm, thermodynamic, and kinetic study, Int. J. Environ. Anal. Chem., 103 (2023) 2223–2239.

[33] A. Sheikhmohammadi, B. Hashemzadeh, A. Alinejad, S.M. Mohseni, M. Sardar, R. Sharafkhani, M. Sarkhosh, E. Asgari, A. Bay, Application of graphene oxide modified with the phenopyridine and 2-mercaptobenzothiazole for the adsorption of Cr(VI) from wastewater: optimization, kinetic, thermodynamic, and equilibrium studies, J. Mol. Liq., 285 (2019) 586–597.

[34] M.H. Dehghani, A. Zarei, A. Mesdaghinia, R. Nabizadeh, M. Alimohammadi, M. Afsharnia, Adsorption of Cr(VI) ions from aqueous systems using thermally sodium organo-bentonite biopolymer composite (TSOBC): response surface methodology, isotherm, kinetic, and thermodynamic studies, Desal. Water Treat., 85 (2017) 298–312.

[35] S. Chatterjee, S. Mahanty, P. Das, P. Chaudhuri, S. Das, Batch adsorption and process optimization for sequestration of Cr(VI) from aqueous solution using biofilm forming filamentous fungus *Aspergillus niger* BSC-1, J. Water Process Eng., 50 (2022) 103325, doi: 10.1016/j.jwpe.2022.103325.

[36] R. Khosravi, M. Fazlzadehdavil, B. Barikbin, A.A. Taghizadeh, Removal of hexavalent chromium from aqueous solution by granular and powdered *Peganum harmala*, Appl. Surf. Sci., 292 (2014) 670–677.

[37] H. Ma, J. Yang, X. Gao, Z. Liu, X. Liu, Z. Xu, Removal of chromium(VI) from water by porous carbon derived from corn straw: influencing factors, regeneration and mechanism, J. Hazard. Mater., 369 (2019) 550–560.